JOURNAL OF SPACECRAFT AND ROCKETS
Vol. 46, No. 6, November–December 2009

Experimental Results for Communications Blackout Amelioration Using Crossed Electric and Magnetic Fields

Kristina M. Lemmer,* Alec D. Gallimore,† and Timothy B. Smith‡
University of Michigan, Ann Arbor, Michigan 48109
and
Christopher N. Davis§ and Peter Peterson¶
ElectroDynamic Applications, Inc., Ann Arbor, Michigan 48105

DOI: 10.2514/1.45490

As a vehicle reenters the atmosphere or travels at hypersonic speeds within it, a bow shock forms around the leading edge of the vehicle. The air is superheated as it passes through the shock wave and becomes ionized. This plasma layer prevents the transmission of radio frequency communications to or from the vehicle, causing what is know as communications blackout. In this paper, we present results from experiments performed to evaluate the use of crossed electric and magnetic fields to lower the plasma density in a region surrounding an antenna. Plasma number density, plasma frequency, and signal attenuation measurements were made with a Langmuir probe, hairpin resonance probe, and S2-1 probe, respectively. The hairpin resonance probe and the S2-1 probe measured frequency responses for input frequencies ranging from 200 up to 4000 MHz. Results show that this approach is a viable method for communications blackout amelioration. We found that the plasma number density decreases by as much as 70% with the operating conditions used in this work, and the plasma frequency dropped by as much as 75%. The increased reduction in the plasma frequency, as compared to the plasma number density, was due to the addition of greater magnetic field strength when the frequency measurements were made. In addition, frequencies that were previously attenuated by more than 10 dB have almost no attenuation after the application of the electric and magnetic fields.

Nomenclature

A_p	=	Langmuir probe area, m^2
a	=	hairpin probe wire radius, m
$\boldsymbol{B}$	=	magnetic field vector, T
b	=	hairpin probe space-charge sheath thickness, m
c	=	speed of light, m/s
$\boldsymbol{E}$	=	electric field vector, V/m
e	=	electron charge, C
f_o	=	hairpin probe vacuum resonant frequency, Hz
f_p	=	plasma frequency, Hz
f_r	=	hairpin probe resonant frequency, Hz
I	=	current collected by Langmuir probe, A
k_B	=	Boltzmann's constant, J/K
L	=	hairpin probe length, m
l_p	=	Langmuir probe length, m
M_e	=	electron mass, kg
M_i	=	ion mass, kg
m	=	mass, kg
$n_{I,o}$	=	ion number density without ReComm System operating, m^{-3}
n_e	=	electron number density, m^{-3}
n_i	=	ion number density, m^{-3}
$n_{i,R/C}$	=	ion number density with ReComm System operating, m^{-3}
r_i	=	ion gyroradius, m
T_e	=	electron temperature, eV
t	=	time, s
V	=	voltage applied to Langmuir probe, V
$\boldsymbol{v}$	=	velocity vector, m/s
V_i	=	ion velocity, m/s
W	=	kinetic energy, J
w	=	hairpin probe width, m
ε	=	dielectric constant
ζ_C	=	hairpin probe sheath correction factor
λ_D	=	Debye length, m
v_R	=	velocity in the radial direction, m/s
v_{gc}	=	guiding center velocity, m/s
$v_\perp$	=	velocity perpendicular to magnetic field vector, m/s
τ_i	=	end effect parameter

Received 19 May 2009; accepted for publication 28 August 2009.

*Graduate Student Researcher, Plasmadynamics and Electric Propulsion Laboratory, Department of Aerospace Engineering, 1052 FXB Building, 1320 Beal Avenue.

†Arthur F. Thurnau Professor, Plasmadynamics and Electric Propulsion Laboratory, Department of Aerospace Engineering, 3037 FXB Building, 1320 Beal Avenue, Associate Fellow AIAA.

‡Senior Research Assistant, Plasmadynamics and Electric Propulsion Laboratory, Department of Aerospace Engineering, 3041 FXB Building, 1320 Beal Avenue.

§Senior Engineer, 3600 Green Court, Suite 300.

¶Director of Research, 3600 Green Court, Suite 300.

I. Introduction

WHEN a hypersonic vehicle travels through the atmosphere, a bow shock forms in front of the vehicle. As the air passes through the shock, it becomes superheated and ionizes, forming a high-density (10^{15}–10^{19} m^{-3} [1,2]) low-temperature (0.4–1.0 eV [1,2]) plasma layer surrounding the vehicle. The plasma density is high enough such that communication and telemetry signals are prevented from passing to and from the vehicle. Radio frequency signals cannot pass through the plasma layer because the plasma acts as a conductor, blocking transmissions. This causes a condition known as communications blackout. This blackout phenomenon first came to the public's attention when humans began traveling into space and jumped to the forefront of the public eye during Apollo 13's atmospheric reentry from a failed attempted moon landing. When NASA began using the space shuttle for human space travel, and with the addition of the Tracking and Data Relay Satellite (TDRS) system, the communications blackout was no longer an issue for human spaceflight in the United States. Since the orbiter is not fully encapsulated in plasma during reentry, radio signals transmitted to TDRS in orbit are then relayed back down to Earth.

However, with NASA's continuing interest in scientific exploration and sample return missions, communications blackout remains an issue. Also, NASA is retiring the space shuttle and returning to a capsule-type reentry vehicle with the development of the Crew Exploration Vehicle (CEV). This return to a blunt-bodied capsule means that TDRS will no longer be useful in maintaining contact during atmospheric reentry since a capsule is entirely surrounded by plasma. In addition, the U.S. military maintains continual interest in alleviating the blackout problem in order to maintain continuous Global Positioning System (GPS) contact with hypersonic vehicles traveling within the atmosphere.

Passive control and active control methods exist for manipulating the reentry plasma. The most common type of passive control is adjusting the leading-edge geometry of the hypersonic vehicle, also referred to as aerodynamic shaping, in order to allow data transmission through the plasma by weakening the shock strength. One example of aerodynamic shaping is to use a sharply pointed vehicle, which is surrounded by a thinner plasma sheath, as opposed to a more blunted body for reentry [3]. However, sharply pointed vehicles have significantly less payload capacity and more aerodynamic heating issues than more rounded capsules [4].

Active control methods include the addition of electrophilic materials into the flow and plasma manipulation by magnetic fields [5]. When electrophilic materials are injected into the flow upstream of an antenna, the molecules combine with free electrons, creating negative ions and reducing the electron density and therefore the plasma frequency [6]. Although this method is effective in reducing the electron number density by up to 30% (resulting in a plasma frequency reduction of about 50%) [2], the reduction is not sufficient for maintaining communications throughout the reentry process. Increasing the flow rate of the liquid increases the amount of electron number density reduction, but the weight of liquid required to sufficiently lower the plasma frequency to a suitable level (approximately 100 kg [2]) prevents this method from being feasible as the only method for overcoming communications blackout. Therefore, this method would require combination with some other form of density attenuation.

The use of magnetic fields to lower the plasma density shows promise, because binding the electrons tightly to the magnetic field lines prevents them from responding to the electric field component of the electromagnetic oscillation from radio communications [7]. This effectively creates a "window" through which communications can freely pass. However, analytical work has shown that the magnetic field required to allow the communications frequencies of interest to NASA and the U.S. Air Force to penetrate the reentry plasma must be very strong. For example, a 1 T magnetic field would be required to allow S-band frequencies to pass through the plasma layer formed around a vehicle with a very blunt leading edge [8,9]. Although such a strong magnetic field requirement may prohibit the use of this method, the effects of an applied crossed electric and magnetic ($E \times B$) field have not been previously considered in the literature and could lead to some interesting phenomena related to the electron drift, the ion acceleration, and maintaining a strong electric field within an quasi-neutral plasma [10].

The goal of this project is to create a localized region within simulated reentry plasma where the number density is lowered to a level that allows the passage of electromagnetic communications signals. We used a 150-mm-diam helicon plasma source operating with argon to produce plasma densities surrounding an antenna similar to those found during atmospheric reentry. The densities downstream of the helicon source are representative of those found at altitudes ranging from 60 to 75 km for a reentry vehicle on a ballistic trajectory [11]. Plasmas occurring in these conditions typically have frequencies ranging from 280 MHz up to 30 GHz. Then we used electric and magnetic fields produced by the reentry and hypersonic vehicle plasma communication system (ReComm System) to manipulate the plasma and create a region of lower dense plasma within the bulk plasma. Typical reentry plasma layers on ballistic trajectories are approximately 30 mm thick [2], but we were unable to simulate this in the laboratory due to the nature of the thick, uniform helicon source discharge [11]. We compensated for that by only measuring the ReComm System effect on plasma densities within 30 mm of the ReComm System surface.

This paper presents density reduction, plasma frequency, and signal coupling strength measurements from downstream of a 150-mm-diam helicon plasma source and above the ReComm System at the University of Michigan Plasmadynamics and Electric Propulsion Laboratory (PEPL). These results were obtained using a single Langmuir probe, a hairpin resonance probe, and an S2-1 probe, respectively. All probes were operated with both the ReComm System off and on to demonstrate its effect on the plasma.

II. Theory of Plasma Density Reduction Using $E \times B$ Fields

Our idea for the plasma manipulation system most simply consists of crossed magnetic and electric fields forming what is known as an $E \times B$ drift channel for charged particles. This idea has previously shown promise in modeling work done concurrently with this research, demonstrating plasma density reductions of up to a factor of 10 [12]. Using crossed electric and magnetic fields has the potential to provide two means for lowering the plasma density: 1) $E \times B$ drift and 2) the formation of an electrostatic sheath that is stabilized by the magnetic field [12]. The equation of motion for crossed electric and magnetic fields is given in Eq. (1) [13]:

$$m\frac{d\boldsymbol{v}}{dt} = e(\boldsymbol{E} + \boldsymbol{v} \times \boldsymbol{B}) \tag{1}$$

Assuming that an electric field exists along the y axis, a magnetic field along the z axis will cause a moving charged particle to orbit about the z axis while drifting in a circular motion along the x axis. The motion of the charged particle guiding center is described by Chen in Eq. (2) [13] and can be seen in Fig. 1. Thus, if an antenna were placed within the crossed electric and magnetic fields, the general motion of the particles would be in a direction away from it, resulting in a region of lower density from conservation principles:

$$\boldsymbol{v}_{\perp \mathrm{gc}} = \boldsymbol{E} \times \boldsymbol{B}/B^2 \tag{2}$$

Another method by which it is believed that the crossed electric and magnetic fields will create a region of lower number density is by establishing a high-voltage sheath surrounding the antenna that depletes electrons from the region. This concept relies on the fact that because ions are much more massive than electrons, magnetic fields have much more of an effect on electrons than ions. In addition, because strong magnetic fields can be used to stabilize high-voltage sheaths [14], an applied electric field would accelerate ions past an antenna, while the magnetic field traps electrons, preventing arcing between the electrodes used to establish the electric field. The acceleration of the ions again results in the lowering of the plasma density due to conservation principles.

III. Facilities and Experimental Setup

All testing was performed in the Cathode Test Facility (CTF) at PEPL. The CTF is a 2.44-m-long by 0.61-m-diam aluminum-walled vacuum chamber. An attached cryopump is able to evacuate the chamber to a base pressure of 3×10^{-7} torr and can maintain

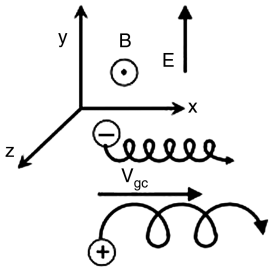

Fig. 1 Particle motion in an $E \times B$ field. The guiding center velocity V_{gc} is known as the $E \times B$ drift velocity [13].

pressures up to 1 mtorr with gas flow. A 150-mm-diam quartz tube surrounded by a double helix, half-wavelength, 13.56 MHz antenna and three electromagnets serves as the helicon plasma source. The source is connected via a rubber O-ring to a 145-mm-diam port on the CTF. Helicon plasma sources create very-high-density (upward of 10^{19} m^{-3}) plasma [15]. The plasma source in this experiment was operated with an argon gas feed such that the background pressure was 0.6 ± 0.05 m torr. Argon was used as the working fluid to simulate the density during atmospheric reentry because the plasma frequency is dependent only on plasma density, not gas species. Moreover, argon requires a lower ionization energy than that required by air. At those conditions the source produces plasma with sufficient ion number density to simulate atmospheric reentry in the upper atmosphere [11].

Figure 2 shows the experimental layout with the indicated axes and directions. Downstream of the helicon plasma source, the ReComm System is located such that its upper surface lies directly below the helicon plasma source port at a vertical (z) position of -85 mm. The measurement origin is located in the radial center of the helicon source at the y position where the quartz tube attaches to the vacuum chamber. As such, the region of interest for these experiments is a small volume defined by the following: $x = -40$ and 0 mm, $y = 350$ and 400 mm, and $z = -75$ and -70 mm.

A. ReComm System Setup

The ReComm System consists of a set of electrodes and an electromagnet to apply crossed electric and magnetic fields, which establish an $E \times B$ drift of charged particles (Fig. 3a). The magnetic field is produced from a custom-designed water-cooled electromagnet made of copper tubing wrapped around an iron core and is set atop an iron base. On top of the electromagnet is a sheet of mica that acts as the surface of a spacecraft. Two stainless steel electrodes set atop the mica sheet provide the electric field. One electrode (cathode) is directly above the center of the iron core and the other (anode) is 40 mm upstream of the first. Figure 3b is a photograph of the ReComm System used in these experiments with the electromagnet, mica sheet, and stainless steel electrodes shown.

Above the iron core of the magnet is a strong (maximum $B_z = 2000$ G) uniform magnetic field along the z axis. However, because of the magnet design, further from the center of the iron core in both the x and y directions, the magnetic field becomes increasingly more divergent. Figure 4a is a plot of the y-z magnetic field strength vector directions and relative magnitudes in a plane along the x axis. The location of the iron core of the magnet is indicated in the figure. In addition, Fig. 4b shows the maximum possible z component of the magnetic field in a plane 10 mm above the ReComm System mica surface. This location is the closest plane that the diagnostic probes could be to the surface of the ReComm System throughout the experiments because of the linear table system used for these experiments and the probe thickness. During ReComm System operation, we varied the peak z component of the magnetic field from 0 to 2000 G, allowing for determination of how variances in the magnetic field strength affected the plasma density. These magnetic fields result in gyro frequencies ranging from about 3 MHz up to 6 GHz.

Perched atop the electromagnet is a 6.3-mm-thick mica sheet. This sheet serves two purposes. The first is to create a dielectric barrier between the plasma and the electromagnet. Without the mica barrier, the plasma, which was at a 50 V-potential [11], would arc to any sharp metal point or edge on the electromagnet. The second is to simulate the dielectric surface of an atmospheric reentry vehicle. Furthermore, atmospheric reentry vehicles must withstand incredibly harsh conditions, including massive heat loads. Dielectric ceramics are among the few materials viable for reentry shielding [16].

The electrodes are made up of 3.2-mm-diam stainless steel rods that run parallel to each other and the x axis, 40 mm apart. Each electrode is set into the mica sheet so that only half of its radius protrudes above the sheet. One-hundred-millimeter lengths of each

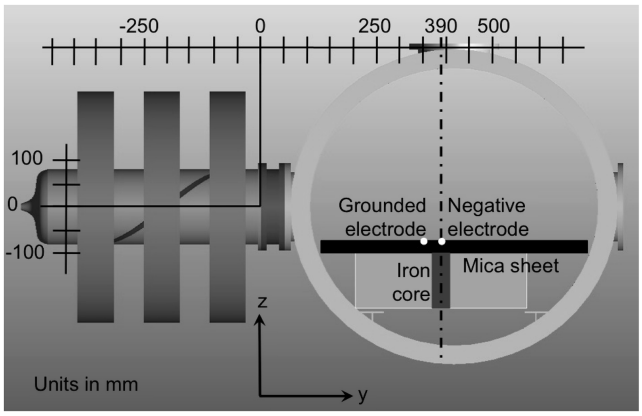

a)

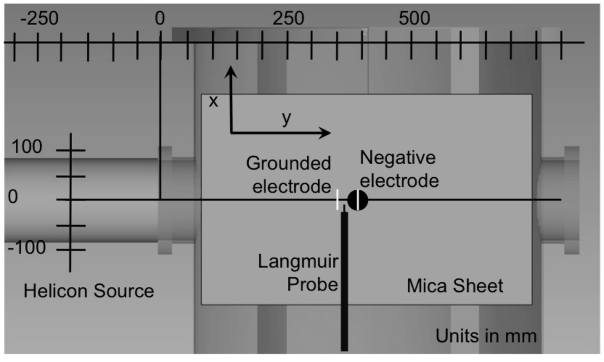

b)

Fig. 2 Experimental layout with indicated (0, 0, 0) measurement point, helicon source location and ReComm System location system setup: a) looking from the positive x direction and b) looking from the positive z direction down onto the surface of the ReComm System.

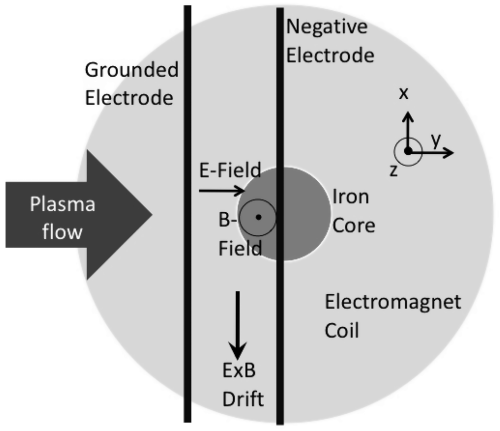

a)

b)

Fig. 3 ReComm System: a) schematic drawing of the layout with indicated directions of electric and magnetic fields along with the direction of the direction of the $E \times B$ drift and b) photograph.

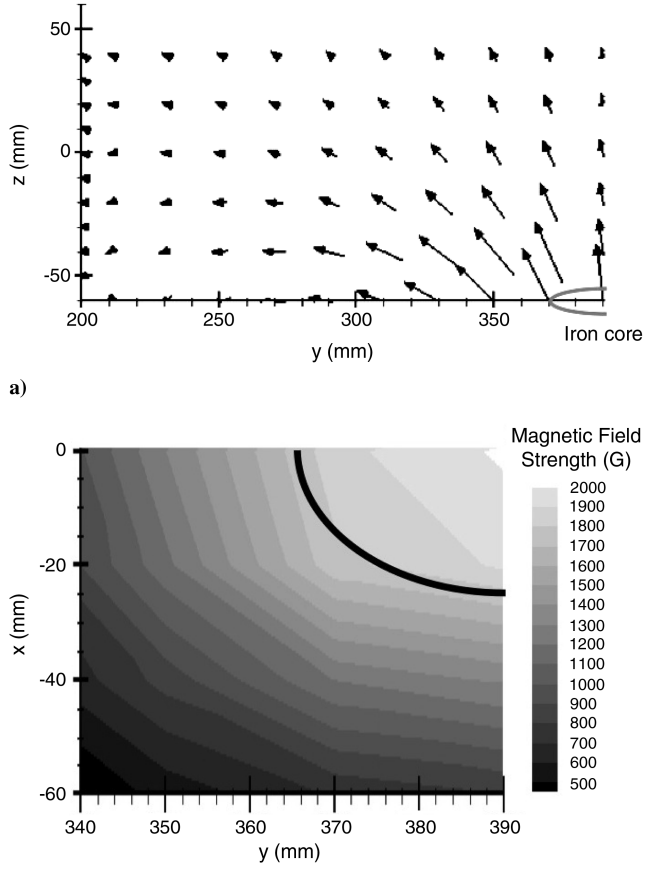

Fig. 4 Measured peak magnetic field of the ReComm System: a) *y-z* magnetic field vectors relative strength and direction in a plane along the *x* axis and b) measured maximum B_z in a plane 10 mm above the ReComm System surface. The white half-oval indicates the location of the iron core of the magnet.

electrode were exposed to plasma, and the remainder of the electrodes were covered with fiberglass tape to hold them in place. The anode is set to ground, and the cathode is set to a potential that varies between 0 V (ground) and −250 V. Thus, the $E \times B$ drift is in the negative x direction, as indicated previously in Fig. 3. Because of limitations of the experimental setup, the maximum operating pressure was 0.6 mtorr. When the pressure was higher, the cryopump would saturate and no longer be able to remove gas from the system. When the pressure was lower, the plasma number density decreased below the threshold established for these experiments. Unfortunately, this limitation meant that the ReComm System was immersed in plasma with neutral pressure at the bottom of the Paschen curve [17]. Therefore, without the presence of a sufficiently strong magnetic field, the electrodes would arc to each other. Operation with only an electric field was not possible, and as the potential between the electrodes was increased, the magnetic field strength had to increase as well to prevent arcing.

B. Diagnostics

We used several plasma diagnostic techniques during this research in order to measure plasma ion number density, plasma frequency, and signal attenuation for various magnetic and electric field settings of the ReComm System. All probes were mounted atop three high-precision linear translation tables to allow for three-dimensional mapping above the ReComm System.

1. Cylindrical RF-Compensated Langmuir Probe

We used a 13.56 MHz RF-compensated Langmuir probe (LP) system from Hiden to measure the plasma number density with and without the ReComm System operating. The LP system consists of a 1.78-mm-long by 0.15-mm-diam tungsten collector, RF circuitry, data acquisition software, and a controller box. The LP controller box produces a varying voltage, and the plasma response is measured by the collected current from the LP tip. The RF circuitry consists of low-pass filters that eliminate any RF noise picked up by the tungsten probe tip as well as a graphite compensation electrode. Raw LP data were stored as current vs voltage characteristics (I–V curves) and then smoothed via a seven-point box-smoothing spline prior to analysis. The smoothing was done to eliminate any 13.56 MHz noise that may be picked up by the transmission lines, therefore facilitating ion number density calculation.

Once the data were smoothed, we analyzed the I–V curves using the cylindrical probe, collisionless sheath analysis, because the mean-free-path-to-probe-radius ratio (Knudsen number) was much greater than unity [18–20]. Also, since the probe-radius-to-Debye-length ratio was less than three for the operating conditions in this experiment [11], the ion number density was calculated using the orbital-motion-limited (OML) assumption based on techniques developed by Laframboise and Parker [21]. This method of analysis assumes that the LP is submersed in cold, collisionless, quasi-neutral, stationary plasma where the sheath dimensions increase as the probe potential increases. This behavior affects the collection of the ion current. Equation (3) shows how the ion number density was calculated:

$$n_i = \frac{1}{A_p}\sqrt{\frac{2\pi M_i}{1.27e^3}\left(\frac{dI^2}{dV}\right)} \tag{3}$$

Strong magnetic fields can affect LP current collection by constraining the motion of charged particles, altering the I–V characteristic [22,23]. Since operation occurred in the OML regime and we were only interested in the ion number density measurements, we had to worry only about the ion saturation region of the I–V characteristic. To ensure that the ion number density calculation remained unaffected by the strong (up to 2000 G) magnetic field generated by the ReComm System, we found the ion gyroradius from Eq. (4), where the electron temperature in the area of interest was no less than 0.5 eV [11]:

$$r_i \text{ cm} = \frac{M_i v_\perp}{|z|B} \approx \frac{2.38\sqrt{T_e}}{B}\sqrt{\frac{M_i}{M_e}} \tag{4}$$

As long as the ion gyroradius was larger than the probe radius (for this case, the ion gyroradius was at least 30 times the probe radius), the ion number density calculation presented above is valid. In addition, the effect of a magnetic field on a cylindrical LP is minimized when the probe axis is perpendicular to the magnetic field lines [24], as it was in the area of interest in these experiments. One final check to ensure the applicability of the OML method for the LP analysis was to check that the ion current to the probe was on the order of the square root of the probe voltage. This is valid and can be seen in Fig. 5, in which Fig. 5a is the ion current from an LP trace where there was no magnetic field present, and Fig. 5b is the ion current from an LP trace where there was a 1850 G magnetic field present.

Another issue that can complicate LP characteristic interpretation is the end effect caused by probe submersion in flowing plasma. End effects are minimal if the parameter given in Eq. (5) below is much greater than unity [25]. Since this was the case for these experiments, our Laframboise and Parker method for analysis is accurate:

$$\tau_l = \frac{l_p}{\lambda_D}\frac{(k_B T_e/M_i)^{1/2}}{V_i} \tag{5}$$

Although traditional LP error estimates for the absolute value of the ion number density are large (∼50%), the relative error between points should be consistent, since the experimental setup and method of analysis remained constant throughout. Thus, the relative trends in which we are interested should be accurate to within 15% [26].

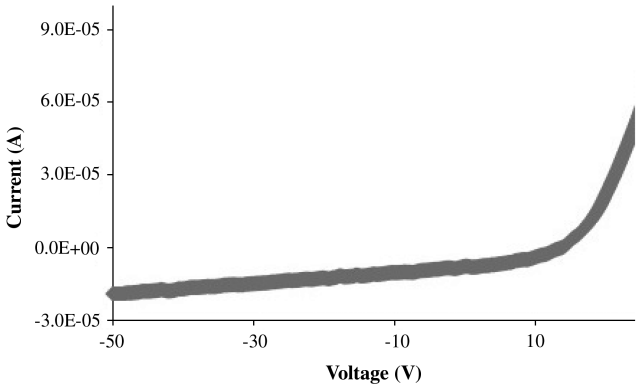

a)

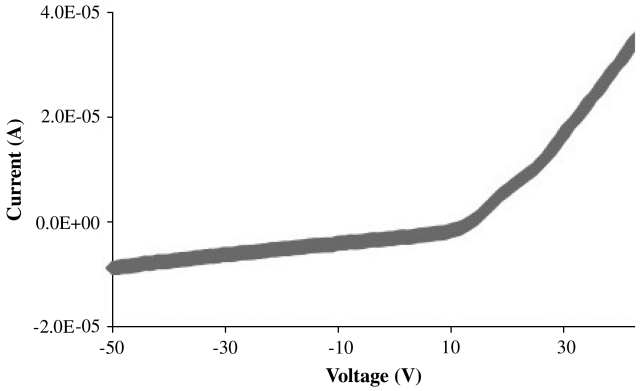

b)

Fig. 5 Ion collection regime of LP probe traces showing that the OML method for analysis is valid for a) no magnetic field and b) 1850 G magnetic field created by the ReComm System magnet.

2. Hairpin Resonance Probe

In addition to the Langmuir probe measurements, we used a hairpin resonance probe to measure plasma frequency for various ReComm System operation conditions. Resonant probes measure the resonant frequency of the hairpin, which is related to the dielectric constant of the surrounding medium by Eq. (6) [27]:

$$f_r = \frac{c}{4L\sqrt{\varepsilon}} \tag{6}$$

Equation (7) relates the dielectric constant, the plasma frequency, and the probe resonant frequency in plasma with little or no magnetic field effects:

$$\varepsilon = 1 - \frac{f_p^2}{f_r^2} \tag{7}$$

Thus, by measuring the shift in the resonant frequency of the hairpin probe, the plasma frequency is obtained. We used a network analyzer to drive a low-amplitude, frequency-varying current to the probe. The power was coupled to the hairpin through an induction loop in a coaxial cable. Reflected power was observed using the same network analyzer in order to determine the frequency shift of the probe. The resonant frequency of the hairpin probe was the frequency at which the reflected power was at a minimum. The frequency components are related as follows:

$$f_r^2 = f_o^2 + \zeta_s f_p^2 \tag{8}$$

$$\zeta_s = 1 - \frac{f_o^2}{f_r^2}\frac{[\ell_n(w - a/w - b) + \ell_n(b/a)]}{\ell_n(w - a/a)} \tag{9}$$

In the above equation, ζ_s is the sheath correction factor, which is based on the dimensions of the hairpin probe and the Debye length of the plasma. The space-charge sheath width b is found by adding the Debye length to the probe wire radius a [28]. Since the Debye length is a function of the plasma number density, and thus the plasma frequency, an iterative process was used to first calculate the plasma frequency and then determine the Debye length. The sheath correction factor varied between 1.1 and 1.5, depending on the plasma density.

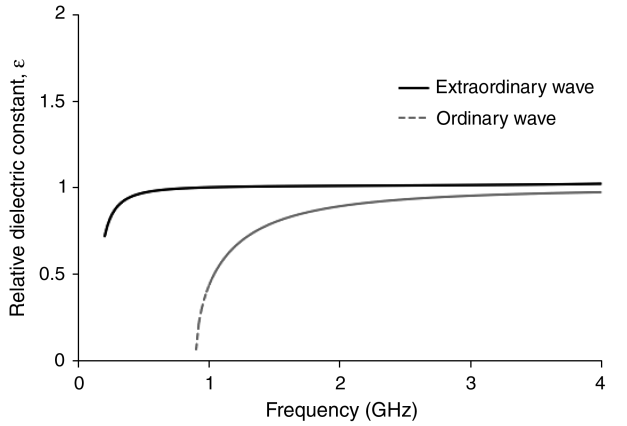

Fig. 6 Relative dielectric constant for the ordinary and extraordinary waves in plasma with $n = 10^{16}$ m^{-3} and $B_z = 2000$ G.

In order to determine whether the magnetic field is strong enough to affect the operation of the hairpin probe, we looked at the plasma dispersion relation for the ordinary wave and the extraordinary wave. For magnetized waves propagating in plasma, the ordinary wave (parallel to the electric field) does not affect the motion of electrons, but the extraordinary wave (perpendicular to the electric field) does [13]. We looked at the relative dielectric constant response for both the ordinary and extraordinary waves in plasma with a number density of 10^{16} m^{-3} and a magnetic field of 2000 G. Figure 6 shows that for the vacuum resonant frequency of the hairpin probe ($\sim$1.5 GHz), the relative dielectric constant is unity. Thus, the resonant frequency shift for our hairpin probe was due only to the ordinary wave allowing the use of Eq. (7) without having to take magnetic field effects into consideration.

The network analyzer used for these experiments has a minimum resolution of 10 MHz; therefore, the error in the resonant frequency measurements is a minimum of ± 5 MHz. In addition, the minimum frequency of the network analyzer is limited to 200 MHz due to the limitations of required RF and dc filters.

3. S2-1 Signal Attenuation Probe

The S2-1 signal attenuation probe uses two monopole antennas submerged in the plasma to measure the coupling strength between them with a vector network analyzer. The benefit of this probe is that it provides a direct measurement of signal attenuation by the plasma. In addition, the plasma frequency can be determined from the signal attenuation data as the minimum of the frequency response. The antennas were set 20 mm apart to simulate the thickness of a reentry plasma layer [1,2], and the measurement was normalized to the case with no plasma in order to remove the antenna response from the results. We used the same network analyzer for these measurements as was used for the hairpin resonant probe measurements, so the same frequency resolution and minimum frequency limitations apply.

IV. Results

We gathered density reduction, plasma frequency, and signal attenuation data for various ReComm System operating conditions. Density reduction was calculated from the LP I–V curves and is presented as the percent that the density decreased when the ReComm System was operating with respect to the density without the ReComm System operating:

$$\%\ \text{reduction} = \frac{n_{i,o} - n_{i,R/C}}{n_{i,o}} \times 100 \tag{10}$$

Table 1 Maximum allowable potential difference between electrodes

Peak B_z, G	Max operating potential, V
0	0
925	100
1385	100
1850	250
2000	250

The plasma frequency was found from data gathered with the hairpin resonance probe, and signal attenuation was measured in dB as a function of frequency with the S2-1 probe. The ReComm System was operated with only the magnetic field and with both the magnetic and electric fields. During electric field operation, there was a maximum allowable potential difference that could be applied between the electrodes for each magnetic field strength operating condition, due to the onset of arcing. These maximum potentials are shown in Table 1.

A. Density Reduction

We measured density reduction as a function of x and y positions and ReComm System operating conditions. The data were obtained in two x-y planes: 1) along the $z = -70$ mm axis, 15 mm above the mica surface (Figs. 7 and 8) and 2) along the $z = -75$ mm axis, 10 mm above the mica surface (Figs. 9 and 10).

Figure 7 was obtained while the maximum magnetic field along the z axis (B_z) was 950 G for two cathode voltage settings: $V_c = 0$ and -100 V. The black curves in Fig. 7 represent the quarter-circle where the data overlap the iron core of the magnet, and the black lines on either side of the plots indicate the location of the electrodes. The region of greatest density reduction (50% less density than what was observed without the ReComm System operating) occurred within the iron core and nearest the cathode. As expected, the crossed electric and magnetic fields caused a reduction in the plasma density. However, with only an applied magnetic field, there was also significant density reduction. In fact, the addition of the electric field seemed only to increase the area where the 50% density reduction occurred. One explanation for this is that since the magnet used in this investigation creates a divergent magnetic field, the field lines trapped the electrons before they could enter the region where the electric field was present. Another possibility is that the electric field was not sufficiently strong with respect to the plasma densities present to cause any significant additional density reduction.

In order to determine whether a stronger electric field provided more density reduction, we increased the magnetic field strength so that the electrodes could not arc to each other. Figure 8 shows the density reduction as a function of x and y positions for maximum $B_z = 1850$ G and for three cathode voltage settings: $V_c = 0, -100$, and -250 V. Similar to the 925 G case, the region of greatest density reduction occurred within the iron core of the magnet and near the negative electrode. The increased magnetic field caused an increase in the density reduction, from 50 up to 55%. As before, the magnetic field alone caused significant density reduction in the plasma, and the addition of the negative 100-V-potential difference across the electrodes increased the density reduction to 60% and increased the size of the region in which the density reduction occurred. However, increasing the cathode voltage to -250 V did not increase the reduction or the size of the reduction window. In actuality, the added voltage caused the maximum density reduction to decrease to 40%, and in locations further from the iron core of the magnet, the ion number density of the plasma actually increased (indicated by a negative density reduction). One possible explanation for this is that the stronger potential difference between the electrodes caused further breakdown of the ionized argon gas, thereby increasing the plasma density. It appears, in the case shown in Fig 8c, that the magnetic field was not strong enough to prevent the dc breakdown in the gas.

We also wanted to determine how the ReComm System affected the plasma closer to the mica sheet. We measured the density

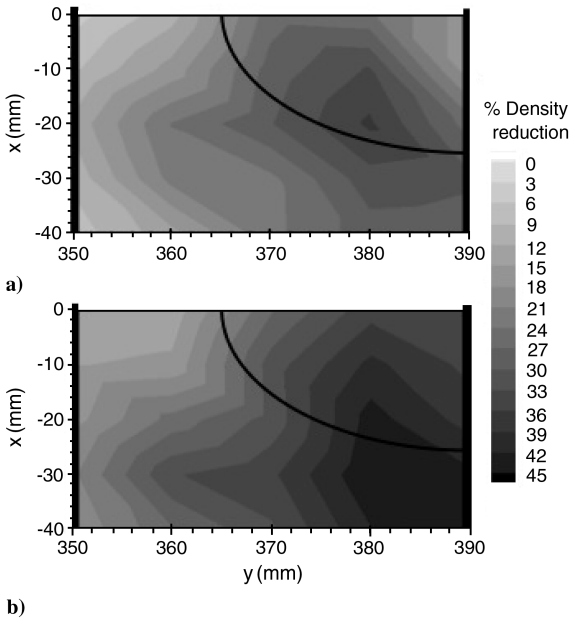

Fig. 7 Density reduction as a function of x and y position along $z = -70$ mm with maximum $B_z = 925$ G for two cathode voltage settings: a) 0 V and b) -100 V. The location of the iron core of the magnet is indicated by the black curves, and the location of the electrodes by the black lines on either side of the plots.

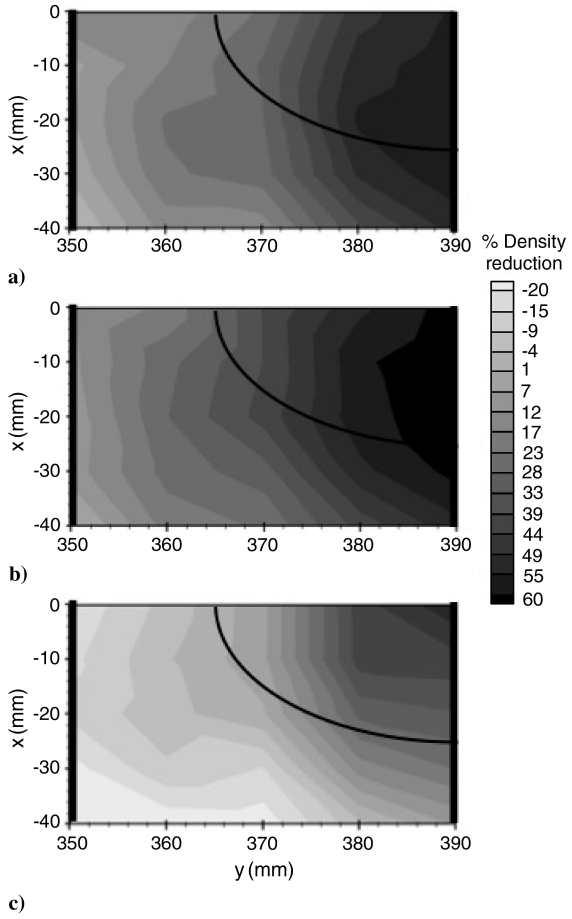

Fig. 8 Density reduction as a function of x and y position along $z = -70$ mm for maximum $B_z = 1850$ G for three cathode voltage settings: a) 0 V, b) -100 V, and c) -250 V. The location of the iron core of the magnet is indicated by the black curves and the location of the electrodes by the black lines on either side of the plots.

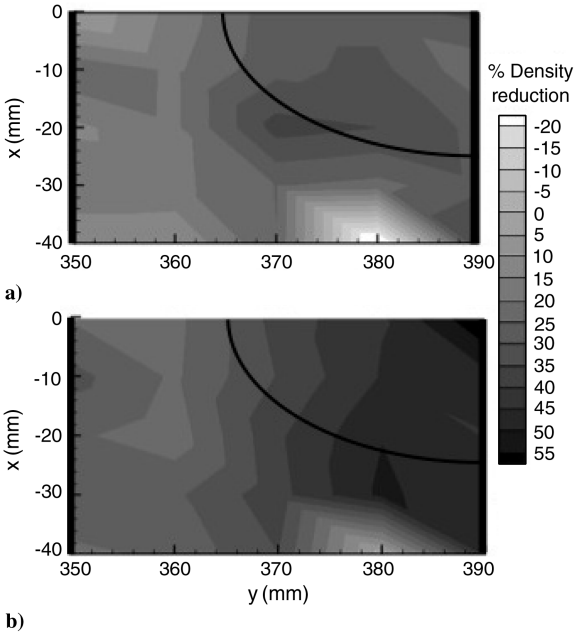

Fig. 9 Density reduction as a function of x and y position along $z = -75$ mm for maximum $B_z = 925$ G for two cathode voltage settings: a) 0 V and b) −100 V. The location of the iron core of the magnet is indicated by the black curves and the location of the electrodes by the black lines on either side of the plots.

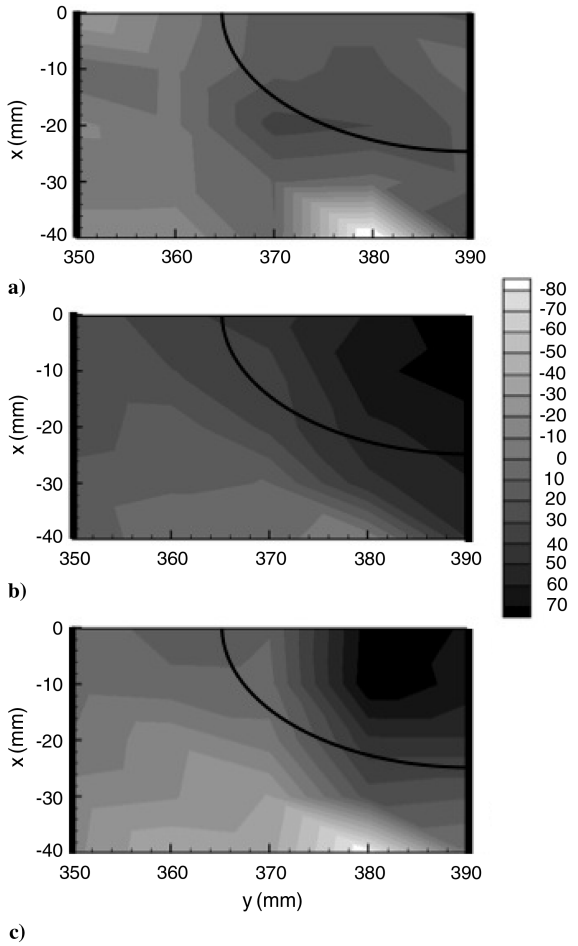

Fig. 10 Density reduction as a function of x and y position along $z = -75$ mm for maximum $B_z = 1850$ G for three cathode voltage settings: a) 0 V, b) −100 V, and c) −250 V. The location of the iron core of the magnet is indicated by the black curves and the location of the electrodes by the black lines on either side of the plots.

reduction when the ReComm System was in use along a plane 10 mm above the mica sheet for the same conditions as shown previously. Figure 9 shows the percent density reduction when 1) $B_z = 925$ G and $V_c = 0$ V and 2) $B_z = 925$ G and $V_c = -100$ V. Since the magnetic field is stronger closer to the surface of the magnet, the overall density reduction along this plane is higher, as expected. Also, in this case the addition of the electric field increased the maximum density reduction from 50 to 55% in addition to increasing the size of the window where the density was reduced. This can be explained by the fact that there was a stronger electric field along this x-y plane since it was closer to the ReComm System. These measurements show that increasing the overall magnetic field strength will increase the thickness of the plasma through which the ReComm System will have an effect.

Increasing the magnetic field strength of the ReComm System further lowered the ion number density to a reduction of 60% without the presence of an electric field. The plasma response to the addition of the electric field with $B_z = 1850$ G in the plane where $z = -75$ mm was similar to that found in the plane where $z = -70$ mm. Increasing the potential on the cathode to −100 V caused a slight increase in the density reduction (up to 70%), but increasing it further to −250 V caused a decrease in the density reduction in the majority of the investigation area. The exception was a small pocket above the iron core of the magnet where the density was still decreased by 70%. This pocket of very low density can be accounted for because this is the location of the strongest magnetic field.

B. Plasma Frequency

We conducted hairpin resonance probe measurements with the ReComm System off and for two operating conditions of the ReComm System: 1) $B_z = 2000$ G and $V_c = 0$ and 2) $B_z = 2000$ G and $V_c = -250$ V.

We found that the plasma frequency decreased significantly when the ReComm System was turned on. The magnetic field alone reduced the frequency by up to 65%, and the addition of the electric field reduced the plasma frequency by 75% of what was present when the ReComm System was turned off (Fig. 11). This was expected based on the LP data, since the plasma frequency is related to the electron number density by Eq. (11) [13]:

$$f_p = \sqrt{\frac{n_e e^2}{m_e \pi}} \tag{11}$$

The 65 and 75% frequency reductions are akin to 80 and 85% density reductions, respectively. When the ReComm System was operating with $B_z = 1850$ G and $V_c = 0$ V, the maximum density reduction was measured as 60% by the LP, and when the potential was increased to −100 V, the reduction increased to 70%. Since the hairpin data were found with a stronger ReComm System magnetic field and electric field, the corresponding increased density reductions were expected. This correlation provides confidence that

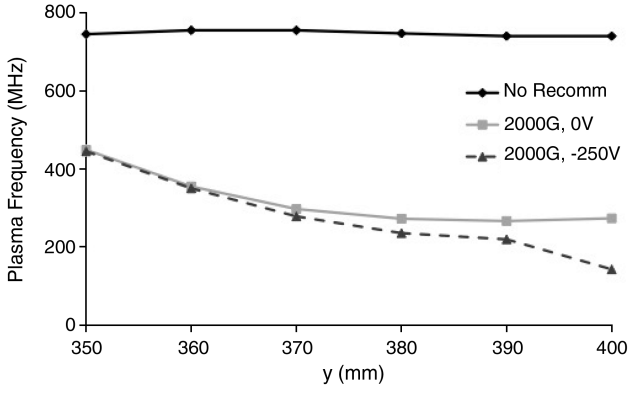

Fig. 11 Plasma frequency measured by the hairpin resonance probe as a function of y position and ReComm System operating conditions.

both the LP and the hairpin resonance probe were properly functioning during testing.

C. Signal Attenuation

We gathered signal attenuation data as a function of input signal frequency for three locations varying from above the anode to above the cathode. We measured the signal attenuation for the same ReComm System operating conditions as were used with the hairpin resonance probe. The minimum of the S2-1 trace corresponds to the plasma frequency. As seen in Fig. 12, turning on the magnetic field greatly lowered the frequency where the communication signal could pass without more than 5 dB of attenuation. The level of frequency reduction was greater in the region closer to the center of the magnet (toward the cathode: Fig. 12c). Adding a potential drop across the electrodes further reduced the plasma frequency at the cathode but had no effect on the plasma near the anode (Fig. 12a). In addition, the change in the minimum of the frequency responses show that the plasma frequency decreases by about 700 MHz at the center of the magnet with the addition of the ReComm System. This finding is consistent with data gathered from the hairpin resonance probe. That a signal was transmitted between the two antennas below the plasma frequency can be explained by the evanescent waves still being able to travel between the antennas. This is because the distance between the antennas is at most 5% (at 1 GHz) of a wavelength, and evanescent waves attenuate as a function of distance rather than the medium through which they travel [13].

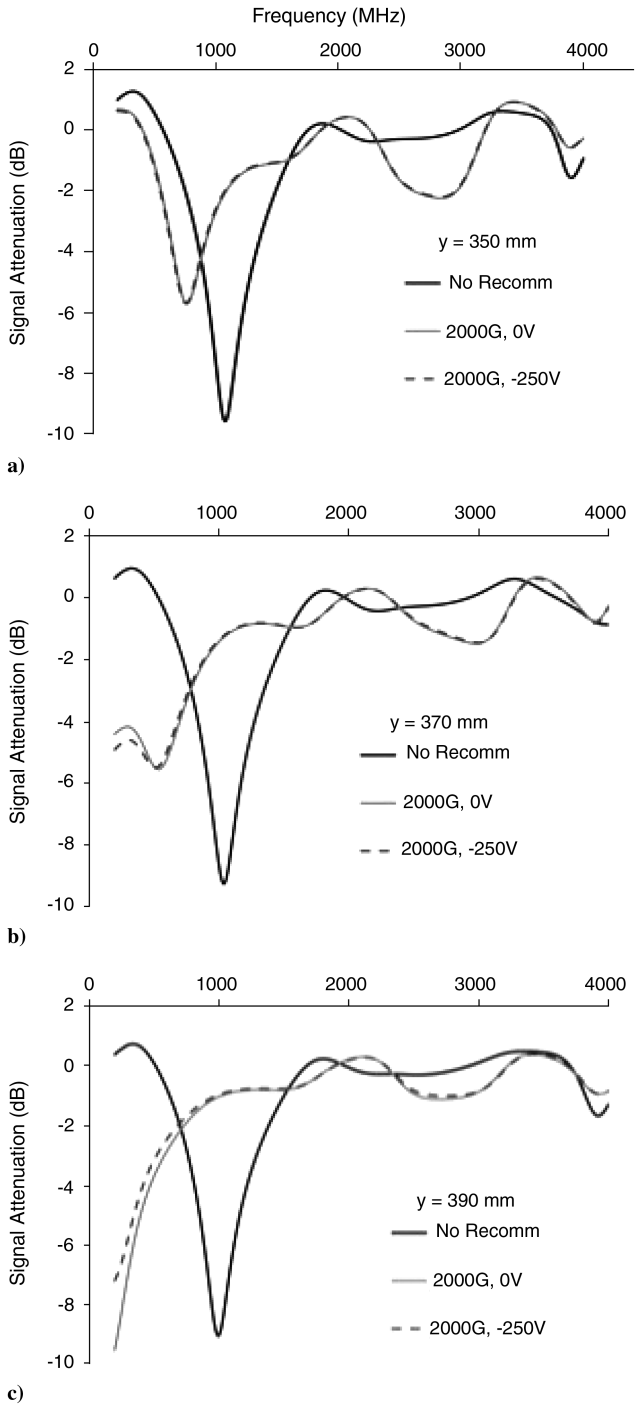

Fig. 12 S2-1 probe signal attenuation as a function of input signal frequency and ReComm System operating conditions for a) $y = 350$ mm (above the anode), b) $y = 370$ mm, and c) $y = 390$ mm (above the cathode).

D. Discussion of Results

Although the ReComm System did not operate as expected, a significant amount of density reduction was still observed. While we initially thought the $E \times B$ drift would be the main cause for the amount of density reduction, the data show that the magnetic field itself is the major contributor to the density reduction. In some cases the ReComm System provided a 70% plasma density reduction. If the magnetic field used in these experiments had been uniform in only the z direction, as was originally planned, the electrons would have been caught in orbits about the magnetic field lines and moved only in the z direction. This would have led to an increase in the electron density in the region above the antenna. Since the magnet used in these experiments did not provide a uniform magnetic field, as shown in Fig. 4, the following equation must be applied to the motion of the charged particles [29]:

$$v_R = \frac{2W_z}{qB_z^2}\frac{\partial B_z}{dz}\hat{y} \tag{12}$$

In the above equation, v_R is the velocity in the radial direction and W_z is the kinetic energy in the z direction. Electrons and ions drift in opposite directions, perpendicular to both the curvature force and the magnetic field lines B. Referring to Fig. 4a, the motion of the electrons in a direction perpendicular to the magnetic field lines would cause them to be deflected away from the region surrounding the antenna. This result is sketched in Fig. 13, where the magnet, electrodes, and electron trajectories are shown. The electron trajectories were generated with the physics-modeling package COMSOL based on the magnetic field strengths used in this experiment. The electrons orbit around the magnetic field lines before drifting away from the region surrounding the antenna.

The electric field contribution seems to be only in the formation of an electrostatic sheath, rather than the contribution of the $E \times B$ drift. Looking at Fig. 7 through Fig. 12, we can see that the any increase in the density reduction with the application of the electric field occurred nearest the cathode. This result implies that the potential

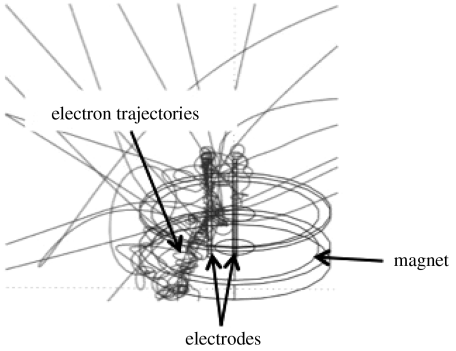

Fig. 13 Expected motion of the electrons with only the magnetic field operating. Image generated by COMSOL physics-modeling package with a magnetic field equivalent to those used in this study. The wire frames of the magnet and the electrodes are shown, and the line traces show the electron trajectories.

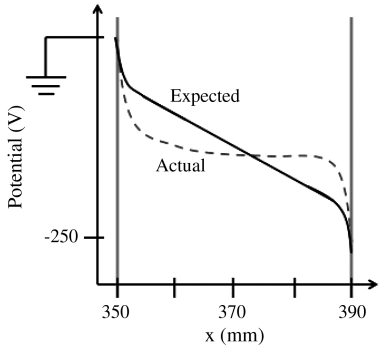

Fig. 14 Expected shape of the potential drop across the electrodes versus what is seen from the data.

drop across the electrodes is not smooth as was originally expected, but consisted of distinct jumps, as shown in Fig. 14. These jumps are indicated by the fact that the only appreciable difference between the data when the electric field was present versus when it was not is at the y location of the charged electrode. Explanations for this result include the fact that the magnetic field is too strong to assume that the ions are not affected by it and that the plasma density, and therefore the collision frequency, is too high to allow for the formation of a smooth potential drop between the two electrodes. Thus, the $E \times B$ drift would be negligible since there is effectively no electric field in the in the central region between the anode and the cathode.

V. Conclusions

The purpose of this research was to determine whether the application of an $E \times B$ field in a plasma sheath could create a region of lower dense plasma through which an electromagnetic wave with a frequency normally below the cutoff frequency would pass through. The experimental results show that plasma density is reduced by as much 70% and the plasma frequency is reduced by as much as 75% with the application of the ReComm System. The slight increase in the plasma frequency reduction from what would be expected by calculation from the plasma density is due to the fact that a higher magnetic field could not be applied while the Langmuir probe was operating. This is due to magnetic field effects. The correlation of the density reduction measured with the LP and the plasma frequency reduction measured with the hairpin resonance probe, and the S2-1 probe allows for confidence in the operation of our probes. The application of a magnetic field significantly reduced the plasma density. The addition of a perpendicular electric field increased the size of the low-density window and further lowered the plasma density slightly in the region near the cathode. This result suggests that the diverging magnetic field played a larger role in the density attenuation than either the $E \times B$ drift or the high-voltage sheath. In addition, we saw signal attenuation levels drop to less than 2 dB for frequencies in the GPS range that were previously attenuated more than 10 dB. Future work should include the creation of a uniform magnetic field, possibly with permanent magnets. This will allow for determination of whether the $E \times B$ field will affect the plasma density to the extent of the diverging magnetic field, or more, as has been suggested by previously performed simulation work [12].

Acknowledgments

The authors would like to acknowledge the support of the U.S. Air Force in funding this work through the Phase-II Small Business Innovation Research grant titled "ReComm—Re-Entry and Hypersonic Vehicle Plasma Communications System," contract FA8718-06-C-0038. Additional funding came from the NASA Constellation University Institutes Project.

References

[1] Grantham, W. L., "Flight Results of a 25,000-Foot-Per-Second Reentry Experiment Using Microwave Reflectometers to Measure Plasma Electron Density and Standoff Distance," NASA Langley Research Center, Hampton, VA, 1970.

[2] Jones, W. L. J., and Cross, A. E., "Electrostatic Probe Measurements of Plasma Parameters for Two Reentry Flight Experiments at 25,000-Feet-Per-Second," NASA Langley Research Center, Hampton, VA, 1972.

[3] Jacavanco, D. J., "Electron Reduction in the Reentry Plasma Sheath," U.S. Air Force Cambridge Research Labs., Cambridge, MA, 1969.

[4] Huber, P. W., and Sims, T. E., "The Reentry Communications Problem," *Astronautics and Aeronautics*, Vol. 2, 1964, p. 30.

[5] Rybak, J. P., "Progress in Reentry Communications," *IEEE Transactions on Aerospace and Electronic Systems*, Vol. AES-7, No. 5, 1971, pp. 879–894. doi:10.1109/TAES.1971.310328

[6] Schexnayder, C. J., "Electron Density Reduction in Re-Entry Plasma Due to Nitrogen Atom Removal," *AIAA Journal*, Vol. 8, No. 2, 1970, pp. 375–377. doi:10.2514/3.5678

[7] Hodara, H., "The Use of Magnetic Fields in the Elimination of the Reentry Radio Blackout," *Proceedings of the Institute of Radio Engineers*, Vol. 49, 1961, p. 1825.

[8] Starkey, R., Lewis, R., and Jones, C., "Plasma Telemetry in Hypersonic Flight," *International Telemetering Conference*, International Foundation for Telemetering, Paper 02-15-2, San Diego, CA, 2002.

[9] Starkey, R., Lewis, R., and Jones, C., "Electromagnetic Wave/Magnetoactive Plasma Sheath Interaction for Hypersonic Vehicle Telemetry Blackout Analysis," 34th AIAA Plasmadynamics and Lasers Conference, AIAA Paper 2003-4167, 2003.

[10] Keidar, M., and Beilis, I. I., "Electron Transport Phenomena in Plasma Devices with $E \times B$ Drift," *IEEE Transactions on Plasma Science*, Vol. 34, No. 3, 2006, pp. 804–814. doi:10.1109/TPS.2006.874852

[11] Lemmer, K. M., Gallimore, A. D., and Smith, T. B., "Using a Helicon Source to Simulate Atmospheric Reentry Plasma Densities and Temperatures in a Laboratory Setting," *Plasma Sources Science and Technology* , Vol. 18, No. 2, 2009, Paper 025019. doi:10.1088/0963-0252/18/2/025019

[12] Keidar, M., Kim, M., and Boyd, I. D., "Electromagnetic Reduction of Plasma Density During Atmospheric Reentry and Hypersonic Flights," *Journal of Spacecraft and Rockets*, Vol. 45, No. 3, 2008, pp. 445–453. doi:10.2514/1.32147

[13] Chen, F. F., *Introduction to Plasma Physics and Controlled Fusion*, Plenum, New York, 1984. doi:10.1063/1.2814568

[14] Keidar, M., Monteiro, O. R., Anders, A., and Boyd, I. D., "Magnetic Field Effect on the Sheath Thickness in Plasma Immersion Ion Implantation," *Applied Physics Letters*, Vol. 81, No. 7, 2002, pp. 1183–1185. doi:10.1063/1.1499516

[15] Boswell, R. W., and Chen, F. F., "Helicons—The Early Years," *IEEE Transactions on Plasma Science*, Vol. 25, No. 6, 1997, pp. 1229–1244. doi:10.1109/27.650898

[16] Rochelle, W. C., Tillian, D. J., Heaton, T. M., Battley, H. H., Murry, L. P., and Grimaud, J. E., "Orbiter TPS Development and Certification Testing at the NASA/JSC 10 MW Atmospheric Reentry Materials and Structures Evaluation Facility," Aerospace Sciences Meeting, AIAA Paper AIAA-1983-147, Reno, NV, 1983.

[17] Burm, K. T. A. L., "Calculation of the Townsend Discharge Coefficients and the Paschen Curve Coefficients," *Contributions to Plasma Physics*, Vol. 47, No. 3, 2007, pp. 177–182. doi:10.1002/ctpp.200710025

[18] Langmuir, I., "The Interaction of Electron and Positive Ion Space Charges in Cathode Sheaths," *Physical Review*, Vol. 33, 1929, pp. 954–989. doi:10.1103/PhysRev.33.954

[19] Chen, F. F., *Plasma Diagnostic Techniques, Electric Probes*, Academic Press, New York, 1965.

[20] Hershkowitz, N., "Chapter 3: How Langmuir Probes Work," *Plasma Diagnostics*, Academic Press, Orlando, FL, 1989, pp. 113–183.

[21] Laframboise, J. G., and Parker, L. W., "Probe Design for the Orbit-Limited Current Collection," *Physics of Fluids*, Vol. 6, No. 5, 1973, pp. 629–636. doi:10.1063/1.1694398

[22] Aikawa, H., "The Measurement of the Anisotropy of Electron Distribution Function of a Magnetized Plasma," *Journal of the Physical Society of Japan*, Vol. 40, No. 6, 1976, p. 1741. doi:10.1143/JPSJ.40.1741

[23] Passoth, E., Kaurdna, P., Csambal, C., Behnke, J. F., Tichy, M., and Helbig, V., "An Experimental Study of Plasma Density Determination by a Cylindrical Langmuir Probe at Different Pressures and Magnetic Fields in a Cylindrical Magnetron Discharge in Heavy Rare Gases,"

Journal of Physics D: Applied Physics, Vol. 30, No. 12, 1997, p. 1763. doi:10.1088/0022-3727/30/12/013

[24] Hutchinson, I. H., *Principles of Plasma Diagnostics*, 2nd ed., Cambridge Univ. Press, Cambridge, England, U.K., 2002. doi:10.1088/0741-3335/44/12/701

[25] Chung, P. M., Talbot, L., and Touryan, K. J., "Electric Probes in Stationary and Flowing Plasma Part 1: Collisionless and Transitional Probes," *AIAA Journal*, Vol. 12, No. 2, 1974, p. 133. doi:10.2514/3.49183

[26] Foster, J. E., "Intercusp Electron Transport in an NSTAR-Derivative Ion Thruster," *Journal of Propulsion and Power*, Vol. 18, No. 1, 2002, pp. 213–217. doi:10.2514/2.5922

[27] Stenzel, R. L., "Microwave Resonator Probe for Localized Density Measurements in Weakly Magnetized Plasma," *Review of Scientific Instruments*, Vol. 47, No. 5, 1976, pp. 603–607. doi:10.1063/1.1134697

[28] Sands, B. L., Siefert, N. S., and Ganguly, B. N., "Design and Measurement Considerations of Hairpin Resonator Probes for Determining Electron Number Density in Collisional Plasmas," *Plasma Sources Science and Technology* , Vol. 16, No. 4, 2007, pp. 716–725. doi:10.1088/0963-0252/16/4/005

[29] Lieberman, M. A., and Lichtenberg, A. J., *Principles of Plasma Discharges and Materials Processing*, Wiley, New York, 1994. doi:10.1002/0471724254

A. Ketsdever
Associate Editor